

# Quantization of human motions and learning of accurate movements

E. Burdet, T.E. Milner

School of Kinesiology, Simon Fraser University, B.C., B5A 1S6 Canada

Received: 15 May 1997 / Accepted: 5 December 1997

**Abstract.** This paper presents a mathematical model for the learning of accurate human arm movements. Its main features are that the movement is the superposition of smooth submovements, the intrinsic deviation of arm movements is considered, visual and kinesthetic feedback are integrated in the motion control, and the movement duration and accuracy are optimized with practice. This model is consistent with the jerky arm movements of infants, and may explain how the adult motion behavior emerges from the infant behavior. Comparison with measurements of adult movements shows that the kinematics of accurate movements are well predicted by the model.

---

## 1 Introduction

### 1.1 Motivation

Human arm movements are smooth, have generally symmetrical velocity profiles, and can be described well using mathematical models maximizing smoothness (Flash and Hogan 1985; Uno et al. 1989). A close examination of arm movements of infants (von Hofsten and Roennqvist 1993) and accurate arm movements of adults shows that the movement is, however, segmented in submovements (Milner and Ijaz 1990; Milner 1992). With increasing accuracy the velocity profile of adult movements also becomes increasingly asymmetrical.

The work described in this paper was motivated by these features of human arm movements, which are not well captured by existing models. We investigated how humans adapt their behavior in order to perform accurate movements. We did it in the constructive way: by realizing a model of this learning.

### 1.2 Review of the literature

For more than 100 years, reaching movements have been studied in order to infer the visual and motor control of arm movements (Woodworth 1899; Fitts 1954; Georgopoulos 1986; Jeannerod 1988). Woodworth (1899) performed some of the first quantitative experiments and found that the movements are composed of two phases: an approach phase followed by an adjustment phase. Fitts et al. (1954) investigated the speed/accuracy trade-off. Subjects were instructed to perform reaching movements as fast and precisely as possible, and the movement time and accuracy were recorded. Fitts observed that the movement time is a linear function of the logarithm of the movement amplitude divided by the movement duration. This mathematical relation, called Fitts' law, is reproduced by the model of Crossman and Goodeve (1983). According to this model the movement is composed of a sequence of submovements not overlapping in time, and each submovement progresses half of the remaining distance to the target. Schmidt (1979) found that in very fast movements directed to the same end location, the end position has a standard deviation around the target position proportional to the amplitude divided by the duration, i.e., to the mean velocity. The variation of the trajectory during repeated movements has been measured in many studies (Georgopoulos 1986; Paulignan et al. 1991a,b; Shadmehr and Mussa-Ivaldi 1994).

In the model of Meyer et al. (1988, 1990) the movement is composed of a sequence of submovements not overlapping in time, as in the model of Goodeve. Corresponding to the finding of Schmidt, the amplitude of each submovement is a Gauss-distributed random variable with standard deviation proportional to the mean velocity of this submovement. The mean amplitude of the submovements is determined such that the time of the overall movement is minimized. The resulting mathematical law generalizes Fitts' law: for an increasing number of submovements Meyer's law converges to Fitts' law.

In Meyer's model, each submovement ends before the next submovement begins. This is not consistent with the

---

Correspondence to: E. Burdet (e-mail: e.burdet@ieec.org, <http://www.sfu.ca/~eburdet>)

movement kinematics measured by Milner and Ijaz (1990). In their experiment, subjects moved a peg into a hole 0.2 m away, for holes of four different diameters. They found that the motion velocity is modulated with the hole diameter, and the velocity profile has small oscillations (Fig. 1). Using these measurements, Milner showed that the movement can be represented well as the superposition of smooth submovements (Milner 1992), as proposed previously by Morasso (1981; Flash and Henis 1991; Henis and Flash 1995). Milner further suggested that these submovements correspond to visual corrections. The hypothesis that human movements are composed of discretely generated submovements is consistent with many experiments (Woodworth 1899) Langolf et al. 1976; Abend et al. 1982; Crossman and Goodeve 1983; Vallbo and Wessberg 1993).

Several other models of reaching movements have been proposed recently (Bullock et al. 1993; Hirayama et al. 1993; Plamondon 1995a,b). The trajectories generated using these models have smooth velocity profiles and reproduce the speed/accuracy trade-off found in human movements. In all these models, however, the velocity profiles have qualitative differences with the profiles measured by Milner. In particular, the small oscillations are not reproduced. In addition, the models of Plamondon (1995a, b) and Kawato (Hirayama et al. 1993), as well as Meyer's model, do not consider the visual feedback.

Hoff (1992) used optimal control theory to model the control of reaching movements. He formulated the motion planning as a second-order linear feedback system with the jerk as control variable, and required that the movement minimizes the integral of the square of the jerk. Using this model, he could simulate reaching movements with final accuracy constraints and pertur-

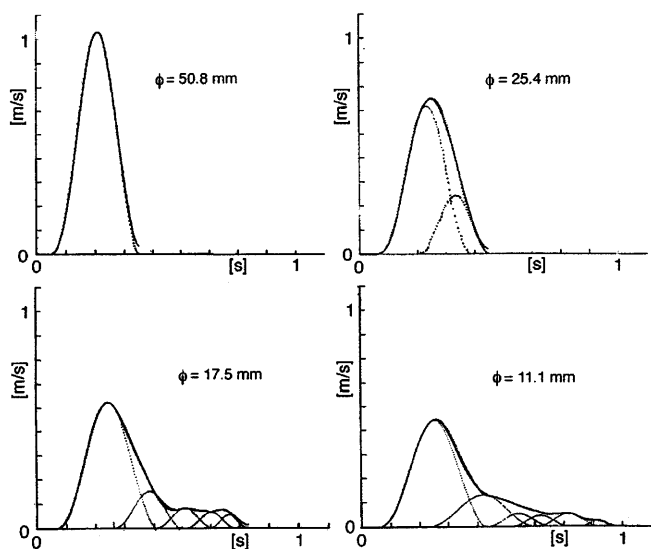


**Fig. 1.** Velocity profile of movements measured by Milner and Ijaz (1990), where subjects had to place a peg into one of four holes of different diameters  $\phi$ . As one can see, the movement kinematics depends on the required accuracy. The overall velocity profiles were measured, and the submovements (dotted lines) were simulated using an interactive program (Milner 1992)

bation of the target position. Some facts, however, speak against this model: it is continuous, which is not consistent with the discrete nature of motions found previously (Langolf et al. 1976; Schmidt 1979; Abend et al. 1982; Milner et al. 1990; Milner 1992); the kinematics of movements with perturbation of the target position are better reproduced with a model where the movement is the superposition of two submovements: one from the start to the first target and the second from the first to the second target (Flash and Henis 1991; Henis and Flash 1995); the analytical calculations are complex and must be completed numerically (Hoff 1992); and finally, the smoothness of human motion may result to a large extent from muscle mechanics rather than from explicit trajectory control (Krylow and Rymer 1997).

'Reaching' movements of infants are saccadic, i.e., composed of submotions. Von Hofsten et al. measured these movements and found that they can be described as a sequence of smooth submovements (von Hofsten 1991). They also observed how infants adapt their movements at about the sixth month from a sequence of nearly equal, well separated submovements, to an asymmetrical velocity profile as observed by Milner and Ijaz for the adult movements, with a large initial submovement followed by a sequence of small submovements.

### 1.3 Aims

In this paper a mathematical model will be presented for the generation of reaching movement by humans. This model is based on the hypothesis that the movement is composed of discretely generated submotions. It considers the intrinsic deviation of arm movements, and feedback from vision and proprioception. It may explain how newborns adapt their reaching strategy to their current capabilities and slowly learn the adult behavior. It also explains how the speed-accuracy trade-off may be solved by adults.

In the models cited above, the movement parameters are calculated analytically, or with a long 'learning phase' that can hardly be related to the way infants learn reaching movements. In contrast, in our model, the adult behavior has to be learned from the infant's behavior in the way the infant learns (von Hofsten and Roennqvist 1993), i.e., by trial and error and in a reasonable number of movements. Qualitative and quantitative predictions of the model will be compared with the movements of infants measured by Von Hofsten (1991) and with the movements of adults measured by (Milner and Ijaz 1990; Milner 1992).

## 2 Model description

Before describing the model, let us introduce two simplifications. First, only the hand trajectory is modeled. The limb and muscle dynamics are not modeled. Second, the movement is modeled in one dimension only. This is partly justified by the fact that

adult hand movements are approximately straight in the (extrinsic) Cartesian space (Atkeson and Hollerbach 1985; Flash and Hogan 1985; Hollerbach and Atkeson 1987; Uno et al. 1989). ‘Goal-directed’ movements of infants are obviously not straight, but the model can easily be generalized to several dimensions. The different hypotheses the model is based upon will now be listed.

### 2.1 Superposition hypothesis and submotion shape

The movement is composed of discretely generated submovements (Figs. 1, 4) (Morasso 1981; Flash and Henis 1992; Milner 1992) which may overlap in time. All the submovements have the same shape. More precisely let

$$x(t), \quad 0 \leq t \leq T \quad (1)$$

be a movement with amplitude  $D$  with a weak accuracy constraint. We consider that this movement is composed of only one submovement (Milner 1992). A movement requiring greater accuracy is assumed to be composed of  $n$  submovements  $x_i$  with amplitude  $D_i$  and duration  $T_i$ ,  $i = 1 \dots n$ . The shape of each of these submotions is determined by

$$x_i(t) = \frac{D_i}{D} x\left(\frac{T_i}{T} t\right), \quad 0 \leq t \leq T_i. \quad (2)$$

As suggested in Milner and Ijaz (1990), the submotion shape is different for each subject, i.e., it is a personalized feature.

### 2.2 Deviation of one submotion

Corresponding to the findings of Schmidt (1979), the amplitude  $D_i$  of each submovement  $x_i$  is a stochastic variable with mean value  $\bar{D}_i$  and standard deviation

$$\sigma_i = C_1 \frac{\bar{D}_i}{\bar{T}_i} \quad (3)$$

where  $C_1$  is a constant with unit seconds. This equation implies that the deviation is proportional to the mean velocity of the submovement.  $C_1$  is identified using (3) with the parameters  $\bar{D}$  and  $\bar{T}$  of movements with weak accuracy constraints (composed of only one submovement).

### 2.3 Movement control

The movement control scheme is depicted in Fig. 2. Vision and proprioception check whether the target is

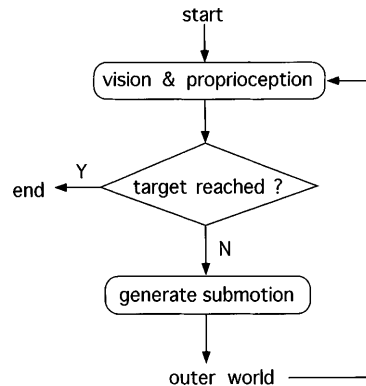


Fig. 2. Control scheme of reaching motions composed of submotions

reached. If not, a new submotion is generated. This is repeated iteratively until the target is reached.

If the submotions do not overlap in time, then the position after each submotion can be directly measured at the end of the submotion. Each submovement is performed independently of the previous one, and a ‘feedback correction’ is performed only after checking the condition ‘target reached?’. Each submovement has an error associated with it (3), but this error can be automatically corrected during execution of the movement because the decision to generate the next submotion relies on sensory information, i.e., information about the actual movement which includes information about the error. Since errors are corrected as the movement progresses an exact plan of the movement is not required prior to its generation.

If a submotion starts before the previous one has been completed, then the position at the end of the first submotion must be inferred while the movement is under way in order to generate an appropriate new submovement. In this case, the movement control is more complex, because each submovement will depend on the previous one.

Figure 3 illustrates this situation. Before starting the movement, a *plan* of the motion corresponding to the desired precision and amplitude is formed and stored in a memory. This plan comprises the amplitudes  $D_i$  and durations  $T_i$  of the submovements of which the movements will be composed. The realized amplitude is not exactly  $D_i$ , but  $\tilde{D}_i \cong D_i$ .  $\tilde{D}_i$  is evaluated using afferent information from vision and proprioception available prior to the onset time of submotion  $x_{i+1}$ . We denote this evaluation as  $D_{(i|i)}$ .<sup>2</sup> The remaining distance to the target is calculated as

$$D_{r,(i|i)} = D_{r,(i-1|i-1)} - D_{(i|i)}. \quad (4)$$

If  $D_{r,(i|i)} \leq 0$ , then the movement is completed; otherwise the next submotion with amplitude

<sup>1</sup> The *mean value*  $\bar{p}$  of a stochastic variable  $p$  is a more intuitive name for the expected value  $E[p]$ .

<sup>2</sup> We use a notation coming from the theory of stochastic processes (Bar-Shalom and Fortman (1988)). The subscript  $(i|i)$  of the estimation  $p_{(i|i)}$  of parameter  $p_i$  indicates that the estimation is performed using all the information available at the time that  $p_i$  must be evaluated, i.e., in our case before the next submotion  $x_{i+1}$  is generated.

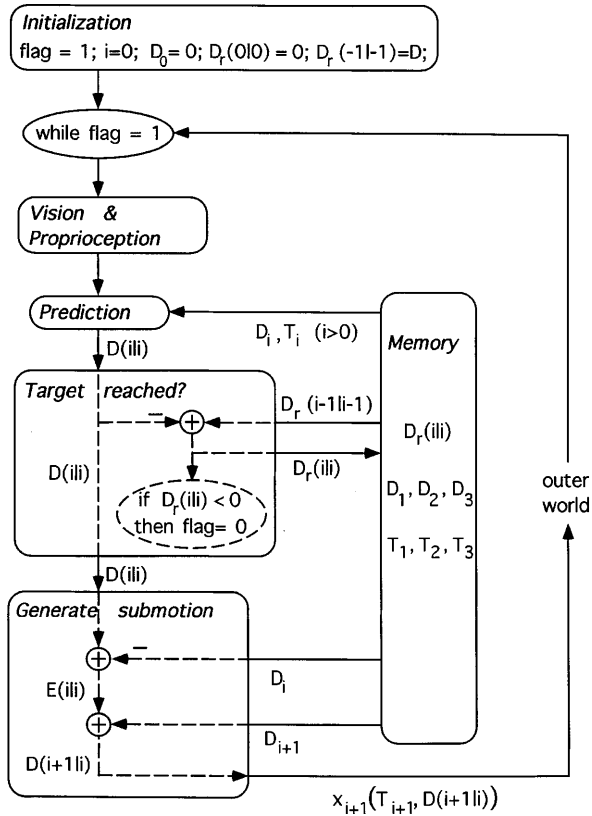


**Fig. 3.** Control scheme of quantized motions when submovements overlap.  $D_i$  and  $T_i$  are respectively the amplitude and duration of the  $i$ th submotion  $x_i$ , and  $D_r(i|i)$  denotes the expectation of the distance to the target at the onset time of submotion  $x_{i+1}$ , given information prior to this time ( $r$  means remaining)

$$D_{(i+1|i)} \equiv D_{i+1} + E_{(i|i)} \quad (5)$$

and duration  $T_i$  is generated.<sup>3</sup> This amplitude is chosen in order to compensate for the difference

$$E_{(i|i)} \equiv D_i - D_{(i|i)} \quad (6)$$

between the planned and realized movement amplitudes.

In summary, when the submovements overlap, a plan and some memory are needed in order to perform accurate movements. The basic strategy, however, remains unchanged (compare Figs. 2 and 3). A biologically plausible algorithm for evaluating the parameters  $D_{(i|i)}$  and  $T_{(i|i)}$  of the current submotion, based on the invariance of submotion shape to time scaling (2), is proposed in the Appendix.

#### 2.4 Timing of the overall motion

The time  $RT_i$  between the start of two consecutive submovements  $x_i$  and  $x_{i+1}$  is proportional to  $T_i$ :

$$RT_i = C_2 T_i \quad (7)$$

<sup>3</sup>  $T_i$  also has a slight error (Schmidt 1979) that must be evaluated. This is performed in the algorithm of the Appendix. For simplicity, however, we neglect this error in the model.

This equation insures that enough time is available for identifying the execution error of the current submotion before the onset of the next submotion, enabling the next submotion to correct for this error. The duration of a movement composed of  $n$  submovements is

$$T = \sum_{i=1}^{n-1} RT_i + T_n \quad (8)$$

In (7),  $C_2$  influences not only the movement duration, but also its precision. Two submovements overlapping in time may have a larger deviation than when they do not overlap, because when they overlap, the execution errors of both submovements are superposed. In this case the execution error of the first submovement cannot be perfectly identified before the second starts.  $C_2$  can, thus, be used to control the deviation of the overall movement.

In order for  $i$ th submotion  $x_i$  to perform an efficient correction, it must not only start after the previous submotion  $x_{i-1}$  has been well identified [as stated by (7)], but it must also start after the submotion  $x_{i-2}$  has been completed (otherwise the parameters of submovements  $x_{i-1}$  and  $x_{i-2}$  could be identified only in combination). Therefore, the following equation is used instead of (7) for calculating the time between the onset of two consecutive submovements:

$$RT_i = \max(C_2 T_i, C_3 T_{i-1} - C_2 T_{i-1}) \quad (9)$$

where  $C_3, 0.5 < C_3 < 1$ , is close to 1.

#### 2.5 Uncertainty of the motion amplitude

Each submovement is performed open-loop, i.e., no correction occurs during a submovement. The correction performed by a submotion is not perfect, because of muscle compliance, because the identification of the current submotion is not perfect, but primarily because of the error brought by this new submovement.

As all the submotion parameters are stochastic variables, the amplitude of the overall movement also is a stochastic variable. The *uncertainty*  $\sigma(t)$  about the current movement is defined as the standard deviation of the prediction of the end position of the current submotion at time  $t$ , when many movements with the same plan have been performed. Generally, the uncertainty about the current submovement should decrease with time, independently of the algorithm used for evaluating the parameters of this submovement. This uncertainty is minimal at the end of the (sub)movement.

The exact evolution of uncertainty during the movement is unknown, although it must be decreasing. In order to simplify its computation, this uncertainty is modeled by a linear decreasing function of the time. Further, it is assumed that each new submovement produces an error independent of the uncertainty at movement onset.

If the movement is composed of only one submotion,  $x_1$ , the uncertainty will be  $\sigma_1 = C_1 D_1 / T_1$ . If the movement is composed of two submovements, then the uncertainty due to the first submotion,  $\sigma_1$ , will decrease linearly with a

factor  $C_4$  until the second submovement onset. At this time,  $RT_1$ , the uncertainty due to the first submotion is

$$(1 - C_4 RT_1) \sigma_1 . \quad (10)$$

The uncertainty due to both submotions at time  $RT_1$  is

$$\sigma = (1 - C_4 RT_1) \sigma_1 + \sigma_2 . \quad (11)$$

For movements composed of only two submotions, this will be the uncertainty at the end position. Similarly, the uncertainty resulting after movements composed of  $n$  submovements is (Fig. 4):

$$\sigma = \sum_{i=1}^{n-1} \max \left( 0, 1 - C_4 \sum_{j=i}^{n-1} RT_j \right) \sigma_i + \sigma_n . \quad (12)$$

We note that the number of submotions  $n$  is neither fixed nor learned during the movements. It simply emerges from the feedback process and the condition that the movement is completed when the remaining distance  $D_{r,(i|i)} \leq 0$  (Fig. 3).

Instead of using equation (12), the uncertainty  $\sigma$  could be determined by performing many movements, using the algorithm in the Appendix to evaluate the submotion parameters and performing a statistical analysis of the final position error. Although this would be more biologically realistic, we chose not to do it because it is computationally intensive and would lead to a similar uncertainty evolution (Figs. 4, A1). We note that in the biological system, the evaluation of the parameters of the current submotions are performed online by the biological hardware, and thus do not require additional computation time.

## 2.6 Motion optimization

The movements cannot be performed at arbitrarily high speed, because the uncertainty grows with movement

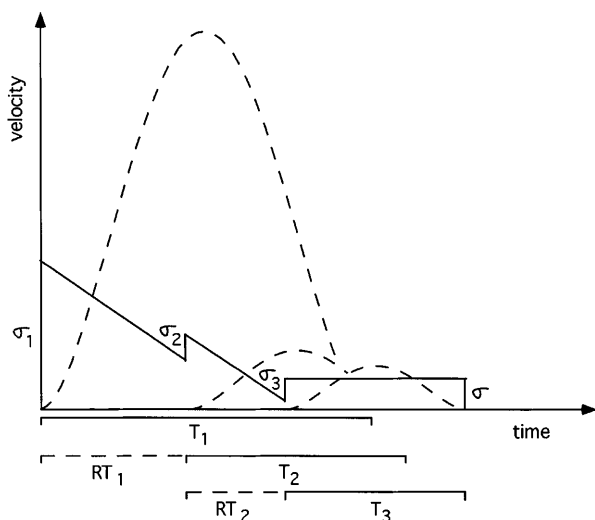


**Fig. 4.** Timing ( $T_i, RT_i$ ) of the different submotions (*dashed lines*) of which a movement is composed, and evolution of the uncertainty  $\sigma$  of the end position of the current submotion (*continuous line*).  $RT_i$  is the time between the onset of submovements  $x_i$  and  $x_{i+1}$

speed [see (3) and (12)]. We assume that humans learn movements optimal with respect to duration and precision by repetition. More precisely, they may learn to correlate movement parameters with the desired accuracy by minimizing the cost function

$$\text{cost} = \text{time} + C_5 \text{uncertainty} , \quad (13)$$

where  $C_5$  is a constant weighting the relative importance of duration and accuracy in the optimization. The submotion parameters providing the fastest movements for a desired accuracy are selected.

The end of the movement is composed of submotions characterized by  $(D_3, T_3)$  which are the smallest possible submotions (Milner 1992; Vallbo and Wessberg 1993). Placing larger and faster submotions at the beginning of the movement results in a higher precision than when they are placed at the middle or the end of the movement. Large submotions would lead to large errors if they occurred near the end of the movement (12). We assume that only the first two submotions [i.e., the parameters  $(D_1, T_1, D_2, T_2)$ ] are optimized. This strategy corresponds to the observation that visually guided motions seem to be composed of an approach phase followed by an adjustment phase (Woodworth 1899; Jeannerod 1988). This also corresponds to a lower cost (13), and may have been learned in a first step.

Using the particular form of the uncertainty in (12), it is possible to calculate the optimal solution analytically. However, this solution would be specific to this equation and could not be applied if the uncertainty function had another shape. For example, using the algorithm in the Appendix, the uncertainty function would be slightly different from (12) and would vary from subject to subject. In addition, humans probably do not compute the optimal solution, but rather learn it with repetition.

## 2.7 Model's parameters

The above model depends on seven constants:  $C_1, \dots, C_5, D_3, T_3$ . These constants are related to movements features and can be unambiguously identified using experimental data. This identification will be described in detail in Sect. 4.1, using the data of (Milner and Ijaz 1990; Milner 1992) to obtain numerical values. How a plan  $(D_1, T_1, D_2, T_2)$  corresponding to a fast and accurate movement to the target is learned by trial and error, will be explained in Sect. 4.2.

## 3 Motion adaptation by infants

This section will examine how the model described above corresponds to the observation of the evolution of reaching movements by infants. It will, in particular, be shown how the planning emerges from experience gained in performing movements.

### 3.1 Experimental observations

We begin by summarizing features of movements of young infants observed by von Hofsten et al. (von Hofsten 1991; van Hofsten and Roennqvist 1993):

- In newborns, the vision capabilities are not yet well developed and the tracking capabilities are very restricted. Force, also, is not yet well controlled (Forssberg et al. 1991).
- The movements of infants until about 6 months of age are formed of approximately equal, well separated submovements (Fig. 5).
- With maturation, both limb control and tracking are improved.
- The speed of all submovements also decreases with maturation.
- At about the sixth month, infants modify their movement patterns from a sequence of approximately equal submotions to an asymmetrical velocity profile characteristic of adult movements (Fig. 5).

### 3.2 Model correlates

**3.2.1 Newborn behavior.** How are these features reflected in the model? A weak movement control, as newborns have [observation (a)], means that  $C_1$ , i.e., the deviation, will be high and  $C_4$ , the factor controlling the decrease of the deviation during the movement, will be small. Poor tracking capabilities also contribute to a small  $C_4$ .

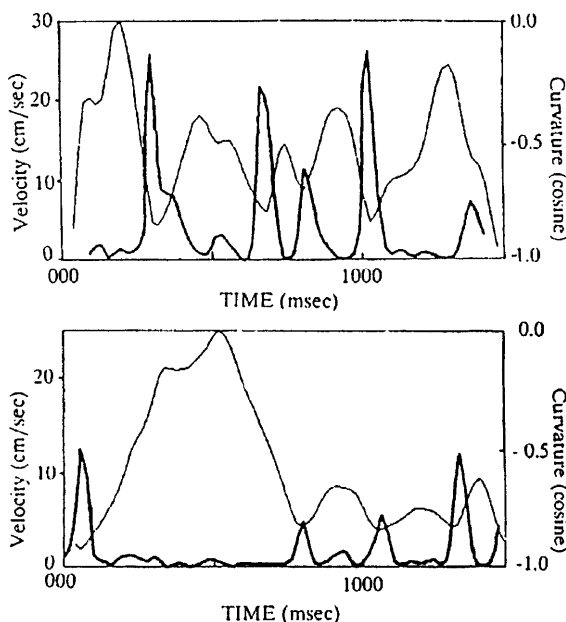


**Fig. 5.** Evolution of the kinematics of reaching movements at about the sixth month (figures from (von Hofsten 1991)). *Above:* velocity profile (*thin line*) and curvature (*thick line*) of a typical movement performed at the age of 19 weeks ( $\cong 4.3$  months). *Below:* the same data at the age of 31 weeks ( $\cong 7$  months). Note the transport phase in the first half of the motion, which generally appears at about 6 months

If there is not enough time between two consecutive submotions, the uncertainty about the end position will increase with each submovement [Eqn. (12)]. This has several consequences:

- It places constraints on  $C_2$ :  $C_2$  must be large enough that the uncertainty does not increase with each submovement.
- With a large  $C_2$ , the movement will be a sequence of submotions rather than a continuous movement. The movement almost stops after each submotion.
- Besides considerations regarding precision, there may be other reasons for the newborn strategy of performing a sequence of well-spaced, approximately equal submotions toward the target. As the uncertainty is not increasing with each submovement, only the parameters of the next submovement need to be known in advance. Using equal submotions makes the planning even more trivial. The infant has only to perform small submotions until the target is reached (Fig. 2). This very simple iterative control strategy, and the fact that in this way almost no experience and no plan are required, correspond to the conditions met by newborns.

**3.2.2 Evolution of movement patterns.** Observation (c) is modeled by an increase in  $C_1$  and a decrease in  $C_4$ . Applying observation (d) to the model will also result in more accuracy [see Eqn. (3)]. The submotions and the overall movement are, thus, becoming more accurate. As they become more accurate the ‘strategy’ of the newborn can be modified in order to minimize the movement duration:

- The submovements may overlap more, i.e.,  $C_2$  can be reduced. The movement will then be more continuous.
- The two first submotions may be larger.

We emphasize that this is not really a new ‘strategy’ (Fig. 3), but emerges from the basic strategy depicted in Fig. 2, as the movement is practiced.

The infant performs many movements. It may observe the duration and precision of each movement and memorize the best movements, i.e., store the submotion parameters minimizing the cost (13). A plan of the movement can be formed, which consists of a set of these parameters whose values depend upon the desired accuracy.

The evolution of infants’ reaching [observation (e)] can be modeled in this way. The infant’s behavior seems to converge to the optimal solution given by our model, i.e., optimization with respect to movement duration and accuracy.

## 4 Speed/accuracy trade-off by adults

The velocity profile of adults depends on the required accuracy. In this section it will be shown how this behavior emerges from experience gained during performing movements.

#### 4.1 Determination of the model parameters

In our model, besides the plan  $(D_1, T_1, D_2, T_2)$ , which can be different for every movement, seven fixed parameters  $D_3, T_3, C_1, C_2, C_3, C_4, C_5$  determine the movement. As the prediction of our model will be compared with the measurements of Milner and Ijaz (1990), the values of these seven parameters will be determined using the kinematic features found in their experiment (Milner and Ijaz 1990; Milner 1992).

First, we specify that more than 95% of the movements to each target hole must be successful. Expressed mathematically, the movement end position is Gauss-distributed with deviation

$$\sigma = \frac{\text{hole diameter}}{4} . \quad (14)$$

The constant  $C_1 = 0.024$  s is determined from Eqns. (3) and (14), using experimental values  $D = 0.207$  m and  $T = 0.383$  s from movements to the largest hole.  $C_2 \equiv 0.45$  and  $C_3 \equiv 0.90$  are computed from statistical analysis of the first submovements. Statistical analysis of the last submotions of movements with high accuracy, i.e., to the two smallest holes, gives  $D_3 \equiv 0.1$  m and  $T_3 \equiv 0.2$  s. In the terminal movement phase composed of minimal submotions  $(D_3, T_3)$ , a new submotion is generated every  $C_2 T_3 = 90$  ms, corresponding approximately to the frequency found in Miall (1996).  $C_4 \equiv 0.008$  is determined such that

$$(1 - C_4 R T_3) \sigma_3 \equiv 0 . \quad (15)$$

This insures that the minimal submotions, following the third submotion, do not increase the uncertainty. The uncertainty (12) then becomes

$$\sigma = (1 - C_4(R T_1 + R T_2)) \sigma_1 + (1 - C_4 R T_2) \sigma_2 + \sigma_3 . \quad (16)$$

Finally,  $C_5$  is tuned so that the maximum velocity of a movement with six submotions corresponds approximately to the mean maximum velocity of movements to a hole of diameter 0.0111 m.

#### 4.2 Movement kinematics

Using (12) for estimating the uncertainty, the parameters  $(D_1, T_1, D_2, T_2)$  were perturbed stochastically. More precisely, after each movement these parameters were modified by a Gauss-distributed perturbation (with  $\sigma_{D_i} = 0.03$  m and  $\sigma_{T_i} = 0.02$  s,  $i = 1, 2$ ). The parameters minimizing the cost (13) and fulfilling the required accuracy were memorized. One thousand movements were performed for each of seven different values of the uncertainty  $\sigma$  between 0.001 and 0.014 m; thus altogether  $7 \times 1000$  learning movements were used.

After this learning phase, the movement duration, time of the maximal velocity and the velocity maxima of the movements corresponding to the different accuracy constraints were computed.

We emphasize that the number of submovements,  $n$ , is not part of the plan. The plan consists only of the

parameters of the first two submotions. The total number of submotions results from these parameters and the control process constituting the movement (Fig. 3). The term  $n$  appears here only because the uncertainty was calculated using (12) rather than using the standard deviation of the endpoint error.

Note that a learning phase of 1000 movements represents roughly a time of 1 h. For learning movements corresponding to different uncertainties, the learning period corresponds to several hours or a few days. This time is not too large and is a possible learning time for humans.

Figure 6 shows that the simulated movement kinematics is qualitatively similar to the experimental kinematics (compare Figs. 1 and 6). As one can see in Fig. 7, the values predicted by the model, while not exactly matching the experimental values quantitatively, do correspond closely to these values. Note that only the parameter  $C_5$  was tuned to adjust the model behavior to the experimental one. Better matching might be obtained by tuning other parameters.

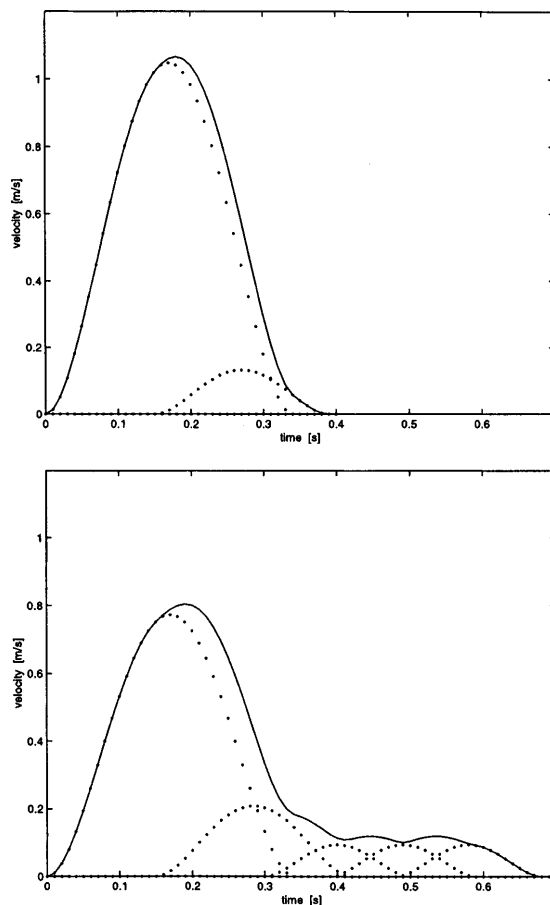


**Fig. 6.** Simulated movements (*continuous lines*) with their submotions (*dotted lines*). Both movements have an amplitude of 0.2 m. The *upper figure* corresponds to an uncertainty  $\sigma = 0.014$  m (corresponding to a hole diameter  $\phi = 0.056$  m in the experiment of Milner and Ijaz 1990) and the *lower figure* to  $\sigma = 0.0072$  m (corresponding to a diameter  $\phi = 0.029$  m)

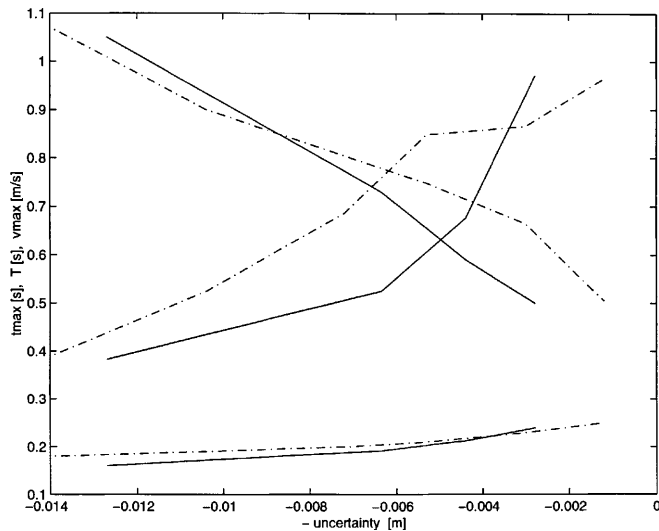


**Fig. 7.** Comparison of predicted (*dashed lines*) with experimental (*continuous lines*) kinematic features. From *top to bottom* are shown: the velocity maxima (curves with negative slopes), the movement duration (curves with positive slopes), and the time of the velocity maxima

#### 4.3 Movement deviation

We also examined the deviation along the movement trajectory. Minimal jerk submovements (Flash and Hogan 1985), with parameters found by optimization, were used to simulate movements. One thousand movements were generated for uncertainties between  $\sigma = 0.001$  m and  $\sigma = 0.014$  m. The submotion amplitudes and durations were stochastically perturbed with a Gaussian distribution and standard deviation corresponding to these parameters. The value of  $\sigma_{D_i}$  was chosen according to (3) with  $C_1 = 0.024$ , i.e., corresponding the results of Milner (Milner and Ijaz 1990; Milner 1992).

$$\sigma_{T_i} = 0.0035 + 0.0572T_i \quad (17)$$

is the least-square estimation of the measurements of Schmidt (1979).

The deviations of movements made to a relatively large hole and a small hole are shown in Fig. 8. We see

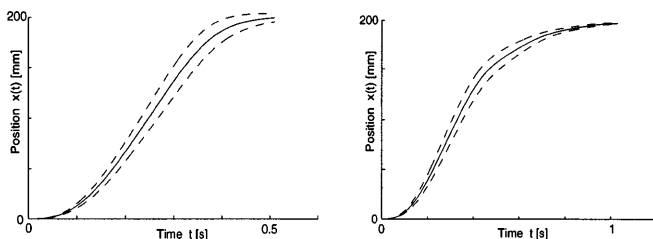


**Fig. 8.** Hand position for movements toward a hole simulated using our model. *Continuous line*, mean, *dashed line*, mean  $\pm$  standard deviation. *Left*: uncertainty  $\sigma = 0.0635$  m corresponding to a hole diameter  $\phi = 0.254$  m in the experiment of (Milner and Ijaz 1998); *right*, uncertainty  $\sigma = 0.0028$  m corresponding to a hole diameter  $\phi = 0.111$  m

there that, as expected, the deviation is larger during the movement and decreases towards its end. This is consistent with experimental findings (Georgopoulos 1981; Paulignan et al. 1991a,b; Shadmehr and Mussa-Ivadi 1994). With increasing accuracy, the deviation becomes smaller at the movement endpoint.

## 5 Discussion

The different hypotheses, results and limitations of the model will now be examined.

*Motion discretization and submotion shape.* Given the phasic and burst-like nature of the activity of many of the output neurons of the motor cortex (Fetz et al. 1980), it is quite possible that there may be discrete activity units at the level of the central nervous system that correspond to the hypothesized submovements of our model. These activity units could be modulated in amplitude and, to a limited extent, in duration as well. However, the principal means of extending the duration of a movement would be by the superposition of a sequence of activity units. The irregularity of unnaturally slow movements (Vallbo and Wessberg 1993; Milner and Ijaz 1990) suggests that they are constructed in this way.

The smoothness of individual submovements probably results from the intrinsic properties of muscles (Krylow and Rymer 1997) and integrating properties of neural pathways. The distinctiveness and similarity of submotion shapes for an individual subject are more likely due to unique characteristics of muscle activation patterns.

Smoothness of the overall movement would be achieved with practice, by adjusting the amplitude and timing of successive submovements by trial and error. Ultimately, the movement could appear very smooth, despite the discrete nature of the underlying command. In our model the smoothness arises from the smoothness of the submotions and their linear superposition (Morasso 1981, 1983). It is neither planned nor built into the cost function. The skilled movements that evolve after months or years of training may represent the outcome of a process in which movements are optimized within the constraints of task goals. Our model suggests that, in contrast to previous findings (Flash and Hogan 1985; Uno et al. 1989; Hoff 1992) smoothness is not directly optimized. Smoothness might rather emerge from the dynamics of muscles and neural pathways and from the minimization of neurophysiologically plausible variables such as muscle activation and movement time.

*Superposition hypothesis.* Our modeling focused on the hand kinematics and neglected the dynamics. For simplicity, only submotion kinematics were used, but the submotions probably correspond to dynamical units of motion. Recent findings suggestive of movement primitives may be related to these units of motion.



Mussa-Ivaldi, Giszter and Bizzi (Bizzi et al. 1991; Mussa-Ivaldi et al. 1994) found that the force fields measured at the endpoint of the frog hindlimb during electrical stimulation of the premotor layers of the gray matter were additive: the force field produced by the simultaneous stimulation of two sites was approximately equal to the sum of the force fields obtained from separate stimulation. Mussa-Ivaldi and Giszter (1992) further suggested that these force fields, characterized by an attractor point, may correspond to movements. The overall movement may be realized by the linear combination of a few 'primitive' force fields. It has also been hypothesized, more generally, that the cortical maps coding the motor control may be represented as a linear function of potential fields with dynamics characterized by an attractor point (Morasso and Sanguineti 1995).

The superposition hypothesis in our model may be related to the linearity of force fields. The movement would arise as the linear superposition of force fields corresponding to submotions. In this view, the submotion of our model would reflect the kinematics resulting from 'force field submotions'.

*Motion timing and sensory feedback.* The hypothesis which we introduced concerning the motion timing (Sect. 2.4) is difficult to verify for human motion. Although we cannot yet test our hypothesis directly, new methods for recording brain activity, such as MEG, may soon provide the means to make the necessary measurements (Conway et al. 1995). As it stands, our hypothesis simply reflects the dependence of accuracy on the amount of overlap between consecutive submotions. It insures that sufficient time will be available to evaluate the outcome of the current submovement.

Examination of movements performed while tracking a moving target suggests that submotions may be generated regularly with a sampling time of about 120 ms or multiples of it (Miall 1996). Such fixed sampling time is incorporated in our model only from the third submotion onward. It could be incorporated into the first two submotions by using the discrete version of (9).

*Duration and accuracy optimization.* The hypothesis that the movement duration and accuracy are optimized during movements, is very powerful. Using seven parameters that can be directly determined from experimental data and tuning only one of these, the model is able to predict the movement kinematics quite well for a large range of endpoint accuracy. It should be noted, though, that a set of parameters different from those determined by the model might result in a lower value of the cost function (Fetz et al. 1980). This is because the model incorporates timing constraints that restrict the search to a small domain of the parameter space so that learning can occur in a relatively short time.

Our model improves on Meyer's model by integrating feedback, generating correct movement kinematics and variation along the movement trajectory. It is also superior to Hoff's model (Hoff 1992) in the sense that it

requires seven parameters instead of eleven, tunes only one of them, does not require any analytical computation, presents a learning scheme consistent with the learning by trial and error observed in humans, and predicts the duration (which was not the case in Hoff's model).

That only the first two submotions are optimized, corresponds to the observation that visually guided motions are composed of an approach phase followed by an adjustment phase (Woodworth 1899; Jeannerod 1988). In this view, the 'plan' for performing movements corresponding to a required accuracy consists of the parameters of the first two submotions. The rest of the movement does not require any plan.

Newborns do not have to possess any plan. Following experience and memorization capabilities, infants may learn a plan during the first 6 months. In our learning scheme, as with infants (von Hofsten and Roennqvist 1993), current actions are learned from past actions. We note that the learning of a motion plan by infants seems to coincide with the appearance of a middle-term memory (Grunwaldt et al. 1960; Hellbruegge 1965).

*Not only a model, but an algorithm.* Generating movements with discrete submovements provides a very economical way of planning smooth movements for machines and computer animated figures (de Boer 1978; Takayama and Kano 1995). Our model explains how a system with continuous feedback and intermittent correction with stereotyped submotions can optimize movements with respect to duration and accuracy. It also provides an algorithm for learning these movements, which can be used for learning optimal motions with a robot guided by a vision system (Brooks 1998; Burdet and Luthiger 1998).

Learning an optimal velocity profile might also be useful for very fast pick-and-place manipulators used in industry. Using common symmetrical velocity profiles, the end-effector oscillates about the movement endpoint for a period of the same order as the time required for the transport phase (Codourey 1991). Asymmetrical velocity profiles have also been shown to minimize these oscillations (Codourey 1991) and thus to minimize the effective movement time. Optimal movements for fast pick-and-place manipulation might be learned using the algorithm described in this paper.

Investigating the strategies of impedance control used by humans during the stabilization phase of goal-directed movements may lead to a more profound insight into the control of these motions and in turn to improved control of fast pick-and-place manipulation.

*Acknowledgements.* We would like to thank Markus Brunner for having programmed the first version of this model, and Tamar Flash and the reviewers for their constructive comments.

## Appendix. Algorithm for estimating the endposition

This appendix proposes a tracking algorithm for a movement composed of superposed stereotyped submovements. The uncer-

tainty at the end of the current submovement can be computed, as will be exemplified for a movement composed of two submotions. The result is similar to the function of (12).

This algorithm is a model of tracking which humans perform using visual and proprioceptive information. It is biologically justified, in the sense that humans possess both an internal model of the motor task (Shadmehr and Mussa-Ivaldi 1994; Shadmehr and Brashers-Krug 1997); i.e., are able to predict the movement trajectory, and the ability to track moving objects (von Hofsten and Roennqvist 1993). Furthermore, identifying the submotions by minimizing the difference between the planned submotion and its realization, as in the following algorithm, is a biologically plausible strategy (Kawato and Gomi 1992; Gomi and Kawato 1992).

Human arm movements are stereotyped (Atkeson and Holterbach 1985). Furthermore, different subjects have reproducible but individual movement patterns (Milner and Ijaz 1990). The following tracking algorithm utilizes the corresponding invariance of the trajectory under time scaling (2).

### A.1 Definitions

Consider a movement  $x(t)$  composed of submotions:

$$x(t) = \sum_{i=1}^n x_i(t - t_i), \quad (\text{A1})$$

where  $t_i$  is the start of the  $i$ th submotion

$$x_i(t) = D_i u\left(\frac{t}{T_i}\right), \quad 0 \leq t \leq T_i \quad (\text{A2})$$

with  $D_i$  and  $T_i$  the amplitude and duration of  $i$ th submotion and  $u$  a normalized submotion, i.e., a movement of unit amplitude performed in a unit time.

Let  $x_1$  be the plan of the first submotion. The actual movement,  $y$ , will be slightly different from  $x_1$ . We assume that  $y$  is a submotion of the same shape as  $x_1$  but with different amplitude and duration:

$$y(t) = I_{(1|t)} + D_{(1|t)} u\left(\frac{t}{T_{(1|t)}}\right). \quad (\text{A3})$$

Let

$$e(t) \equiv y(t) - x_1(t) \quad (\text{A4})$$

be the position error at time  $t$ . The amplitude  $D_{(1|t)}$ , duration  $T_{(1|t)}$  and integral parameter  $I_{(1|t)}$  of a submovement are adapted during the movement to approximate  $y$  by minimizing the squared error,  $e^2$ , at each time.  $I_{(1|t)}$  is a parameter corresponding to constant error.

Once the parameters of the first submotion have been identified, the error relative to the first planned submotion can be corrected by modifying the amplitude of the second submovement. This can be performed iteratively for all subsequent submotions. In this way, it is possible to perform accurate movements despite the intrinsic deviation of submovements.

### A.2 The algorithm

The gradient estimator (Slotine and Li 1991) is used for learning the best estimation of the parameters  $D_{(i|t)}$ ,  $T_{(i|t)}$  and  $I_{(i|t)}$  at time  $t$ . This gives the following algorithm:

$$D_{(i|0)} \equiv D_i; \quad T_{(i|0)} \equiv T_i; \quad I_{(i|0)} \equiv I_i;$$

$$t = RT_{i-1};$$

$$\text{While } t < RT_i \quad \text{Do}$$

$$t = t + dt;$$

$$dD_{(i|t)} \equiv -\gamma_D \frac{\partial(e^2)}{\partial D} \equiv \gamma_D e(t) u\left(\frac{t}{T_{(i|t)}}\right);$$

$$D_{(i|t)} \equiv D_{(i|t-dt)} + dD_{(i|t)};$$

$$dT_{(i|t)} \equiv -\gamma_T \frac{\partial(e^2)}{\partial T} \equiv \gamma_T e(t) u\left(\frac{t}{T_{(i|t)}}\right) \left(-\frac{1}{T_{(i|t)}^2}\right);$$

$$T_{(i|t)} \equiv T_{(i|t-dt)} + dT_{(i|t)};$$

$$dI_{(i|t)} \equiv -\gamma_I \frac{\partial(e^2)}{\partial I} \equiv \gamma_I e(t);$$

$$I_{(i|t)} \equiv I_{(i|t-dt)} + dI_{(i|t)};$$

End (While);

In the above adaptation laws,  $\gamma_D$ ,  $\gamma_T$  and  $\gamma_I$  are positive learning factors.

The above algorithm can be used iteratively for each submotion  $x_i$  from  $i = 1$  to  $i = n$ , i.e., along the entire movement trajectory. Setting  $RT_1 \equiv 0$ , the first integral parameter  $I_{(1|RT_1)}$  will correct for error in determining the beginning of the first submotion. From the second submotion onward, the integral term will correct for the portion of the error of the preceding submotion not yet identified at the onset time of the current submotion.

### A.3 Simulation

This algorithm was tested by simulating many movements composed of different number of submovements. It succeeded in bringing the prediction error to zero at the end of the movement in all cases. This proves that it is able to identify the submotion parameters well.

We now present results for movements of amplitude  $D = 0.200$  m with a standard deviation of the end position  $\sigma = 0.014$  m. The parameters  $(D_1, T_1, D_2, T_2)$  were found by using (12) and performing optimization relative to the cost function of (13). One thousand movements were performed using these parameters. The mean and standard deviation at the end of the current submotion were computed every millisecond.

It turned out that all 1000 movements were composed of two submotions. Figure A1 shows the error in the expectation of the current submotion endpoint for three movements and the mean of this error (the ‘uncertainty’). One sees that the uncertainty is decreasing monotonously with time except at the onset of the second submovement. This curve can be roughly approximated by a stepwise linear function, corresponding to (12).

The simulation of the above algorithm requires the computation of the parameters of each submotion using random generators, the error in each time step and the statistics. To avoid this time-intensive computation, we chose to use (12) for the uncertainty, instead of calculating it as the standard deviation over many movements. With a real biological system most of this computation is not required, because it is implemented in the biological hardware.

### A.4 Practical applications of the algorithm

The above algorithm can be used not only for the model described in this paper, but also for predicting the kinematics of human motions. This may have applications in physiology and teleoperation. For example, recent experiments (Gomi and Kawato 1996) were designed for measuring the muscle impedance at the hand along two-dimensional planar movements. The hand was slightly perturbed during the movement, and stiffness was computed by comparing the perturbed trajectory with the mean trajectory of unperturbed movements of the same duration, with the same start and endpoint.

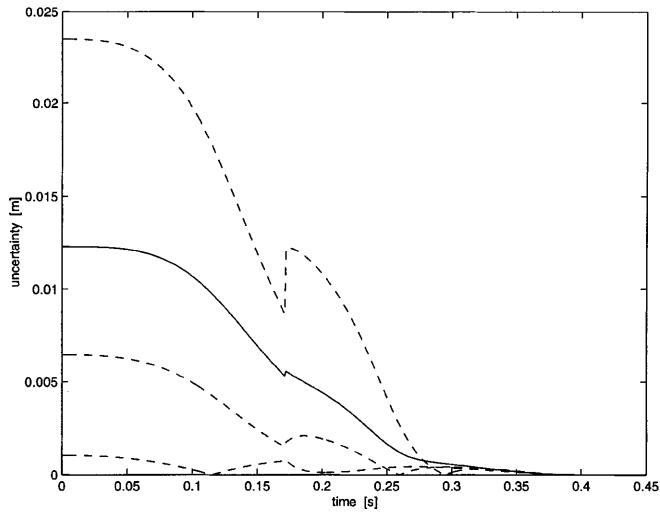


**Fig. A1.** Uncertainty about the endpoint of the current submotion for a movement composed of two submotions. Shown are the uncertainties of three movements performed with different submotion parameters (*dashed lines*), and the mean uncertainty over 1000 movements (*continuous line*).

In general, the current movement (before perturbation) has the same shape as the mean movement, but is scaled relative to it (Milner and Ijaz 1990; Atkeson and Hollerbach 1985). Using the mean trajectory to represent the undisturbed movement without scaling, as was done in (Gomi and Kawato 1996), would result in an error in estimating the muscle impedance. We used real data to show that the above algorithm can be used to scale the parameters of the mean movement trajectory so that it precisely approximates the current movement (Franklin and Milner 1997). Using such a representation of the current movement would greatly reduce the potential for error in estimating muscle impedance. As discussions about neurophysiological hypotheses critically depend on quantitative values of impedance parameters of muscles (Katayama and Kawato 1993), improving the measurement is important for the evaluation of these hypotheses.

## References

- Abend W, Bizzi E, Morasso P (1982) Human arm trajectory formation. *Brain* 105:331–348
- Atkeson CG, Hollerbach JM (1985) Kinematic features of unrestrained vertical arm movements. *J Neurosci* 5:2318–2330
- Bar-Shalom Y, Fortmann TE (1988) *Tracking and data association*. Academic Press, New York
- Bizzi E, Mussa-Ivaldi FA, Giszter SF (1991) Computations underlying the execution of movement. a biological perspective. *Science* 253:287–291
- de Boor C (1978) *A practical guide to splines*. Springer, Berlin Heidelberg New York
- Brooks RA (1998) From earwigs to humans. *Robotics and autonomous systems*, in press
- Bullock D, Grossberg S, Guenther FH (1993) A self-organizing neural model of motor equivalent reaching and tool use by a multijoint arm. *J Cogn Neurosci* 5:408–435
- Burdet E, Luthiger J (1998) Learning the coordination of robot movements with vision processes. *IEEE Trans Robotics Automation*, in press
- Codourey A (1990) Contribution à la commande des robots rapides et précis application au robot Delta à entraînement direct. PhD thesis, Ecole Polytechnique Fédérale de Lausanne, Switzerland
- Conway BA, Halliday DM, Farmer SF, Shahani U, Maas P, Weir AI, Rosenberg JR (1995) Synchronization between motor cortex and spinal motoneuronal pool during the performance of a maintained motor task in man. *J Physiol (Lond)* 489:917–924
- Crossman ER, Goodeve PJ (1983) Feedback control of hand movement and Fitts' law. *Q J Exp Psychol [A]* 35:251–278
- Forssberg H, et al (1991) Development of human precision grip. I. Basic coordination of force. *Exp Brain Res* 85:451–457
- Fetz EE, Cheney PD, Mewes K, Palmer S (1980) Control of forelimb muscle activity by populations of corticomotoneuronal and rubromotoneuronal cells. *Prog Brain Res* 80:437–449
- Fitts PM (1954) The information capacity of the human motor system in controlling the amplitude of movement. *J Exp Psychol* 47:381–391
- Flash T, Henis E (1991) Arm trajectory modification during reaching towards visual targets. *J Cogn Neurosci* 3:220–230
- Flash T, Hogan N (1985) The coordination of arm movement: an experimentally confirmed model. *J Neurosci* 5:1688–1703
- Franklin DW, Milner TE (1997) Using invariant features of voluntary movements to predict hand trajectories. *Society Neurosci Abstr* 23:page 2090
- Georgopoulos AP (1981) Spatial trajectories and reaction times of aimed movements: effects of practice, uncertainty, and change in target location. *J Physiol (Lond)* 46:725–743
- Georgopoulos AP (1986) On reaching. *Annu rev Neurosci* 9:147–170
- Gomi H, Kawato M (1992) Adaptive feedback control models of the vestibulocerebellum and spinocerebellum. *Biol Cybern* 68:105–114
- Gomi H, Kawato M (1996) Equilibrium-point control hypothesis examined by measured arm stiffness during multijoint movement. *Science* 272:117–120
- Grunwaldt E, Bates T, Guthrie D (1960) The onset of sleeping through the night in preschool children. *J Child Psychol Psychiatry* 21:5–17
- Hellbruegge T (1965) Zeitliche Strukturen in der kindlichen Entwicklung. *Monatsschr Kinderentwicklung* 113:252–262
- Henis EA, Flash T (1995) Mechanisms underlying the generation of averaged modified trajectories *Biol Cybern* 72:407–419
- Hirayama M, Kawato M, Jordan MI (1993) The cascade neural network model and a speed-accuracy trade-off of arm movement. *J Mot Behav* 25:162–174
- Hoff BR (1992) A Computational description of the organization of human reaching and prehension. PhD thesis, University of Southern California
- Hollerbach JM, Atkeson CG (1987) Deducing planning variables from experimental arm trajectories: pitfalls and possibilities *Biol Cybern* 56:279–292
- Jeannerod M (1988) *The neural and behavioural organization of goal-directed movements*. Oxford University Press, Oxford
- Katayama M, Kawato M (1993) Virtual trajectory and stiffness ellipse during multijoint arm movement predicted by neural inverse models. *Bio Cybern* 69:353–362
- Kawato M, Gomi H (1992) A computational model of four regions of the cerebellum based on feedback error learning. *Biol Cybern* 68:95–103
- Krylow M, Rymer Z (1997) Role of intrinsic muscle properties in producing smooth movements. *IEEE Trans Biomed Eng* 44:165–176
- Langolf GD, Chaffin DB, Foulke JA (1976) An investigation of Fitts' law using a wide range of movements amplitudes. *J Mot Behav* 8:113–128
- Meyer DE, Kornblum S, Abrams RA, Wright CE (1988) Optimality in human motor performance: ideal control of rapid aimed movements. *Psychol Rev* 95:340–370
- Meyer DE, Smith JEK, Kornblum S, Abrams RA, Wright CE (1990) Speed-accuracy tradeoffs in aimed movements: toward a theory of rapid voluntary action. In: Jeannerod M (ed) *Attention and performance XIII*. Hillsdale, New York pp 173–226
- Miall RC (1996) Task-dependent changes in visual feedback control: a frequency analysis of human manual tracking. *J Mot Behav* 28:125–136

- Milner TE (1992) A model for the generation of movements requiring endpoint precision. *Neuroscience* 49:365–374
- Milner TE, Ijaz MM (1990) The effect of accuracy constraints on three-dimensional movement kinematics. *Neuroscience* 35:487–496
- Morasso P (1981) Spatial control of arm movements. *Exp Brain Res* 42:223–227
- Morasso P (1983) Three dimensional arm trajectories. *Biol Cybern* 48:187–194
- Morasso P, Sanguineti V (1995) Self-organizing body schema for motor planning *J Mot Behav* 27:52–66
- Mussa-Ivaldi FA, Giszter SF (1992) Vector field approximation: a computational paradigm for motor control and learning. *Biol Cybern* 67:491–500
- Mussa-Ivaldi FA, Giszter SF, Bizzi E (1994) Linear combination of primitives in vertebrate motor control. *Proc Nat Acad Sci USA* 91:7534–7538
- Paulignan Y, MacKenzie C, Marteniuk R, Jeannerod M (1991a) Selective perturbation of visual input during prehension movement. 1. The effect of changing object position. *Exp Brain Res* 83:502–512
- Paulignan Y, MacKenzie C, Marteniuk R, Jeannerod M (1991b) Selective perturbation of visual input during prehension movement. 2. The effect of changing object size. *Exp Brain Res* 87:407–420
- Plamondon R (1995) A kinematic theory of rapid human movements. I. Movement representation and generation. *Biol Cybern* 72:295–307
- Plamondon R (1995) A kinematic theory of rapid human movements. II. Movement time and control. *Biol Cybern* 72:309–320
- Schmidt RA (1979) Motor output variability: a theory for the accuracy of rapid motor acts. *Psychol Rev* 86:415–451
- Shadmehr R, Brashers-Krug T (1997) Functional stages in the formation of human long-term motor memory. *J Neurosci* 17:409–419
- Shadmehr R, Mussa-Ivaldi FA (1994) Adaptive representation of dynamics during learning of a motor task. *J Neurosci* 14:3208–3224
- Slotine J-JE, Li W (1991) *Applied nonlinear control*. Prentice-Hall, Rahway, NJ
- Takayama K, Kano H (1995) A new approach to synthesizing free motions of robotic manipulators based on a concept of unit motions. *IEEE Trans Syst Man Cybern* 25:453–463
- Uno Y, Kawato M, Suzuki R (1989) Formation and control of optimal trajectory in human multijoint arm movement. *Biol Cybern* 61:89–101
- Vallbo AB, Wessberg J (1993) Organization of motor output in slow finger movements in man. *J Physiol (Lond)* 469:673–691
- vonHofsten C (1991) Structuring of early reaching movements: a longitudinal study. *J Mot Behav* 23:280–292
- vonHofsten C, Roennqvist L (1993) The structuring of neonatal arm movements. *Child Dev* 64:1046–1057
- Woodworth RS (1899) The accuracy of voluntary movement. *Psychol Rev Monogr Suppl* [1899]